HUMAN GENE THERAPY 22:1137–1142 (September 2011)

DOI: 10.1089/hum.2011.003

Brief Report

Systemic Delivery of a Novel Liver-Detargeted Oncolytic Adenovirus Causes Reduced Liver Toxicity but Maintains the Antitumor Response in a Breast Cancer Bone Metastasis Model

Zhenwei Zhang, Jeffrey Krimmel, Zhiling Zhang, Zebin Hu, and Prem Seth

Abstract

We are interested in developing oncolytic adenoviruses for the treatment of bone metastasis of cancer. A key limitation of systemic delivery of oncolytic adenovirus type 5 (Ad5) is that the majority of the virus is taken up by the liver, causing liver damage and systemic toxicity. Given that Ad5 hexon binding with blood coagulation factor X is a key factor in liver sequestration, and that a rare serotype, Ad48, has a diminished capacity to bind with factor X, we have generated mHAd.luc2, a novel hexon-chimeric oncolytic adenovirus. To create mHAd.luc2, seven hypervariable regions of Ad5 hexon were substituted with the corresponding regions from Ad48. Compared with Ad5-based oncolytic virus Ad.luc2, intravenous injection of mHAd.luc2 into nude mice resulted in significantly reduced liver uptake. A single high dose (1.0×10^{11} viral particles/mouse) of Ad.luc2 resulted in 100% animal death by day 3; whereas none of the mice died in the mHAd.luc2 group. Liver enzyme and liver pathology studies indicated that mHAd.luc2 induced significantly less liver toxicity compared with Ad.luc2. Both mHAd.luc2 and Ad.luc2 exhibited similar binding with breast tumor cells, whereas in the presence of factor X, mHAd.luc2 binding was reduced. Both mHAd.luc2 and Ad.luc2 had nearly equal replication potential in breast cancer cells *in vitro*. Intravenous injection of mHAd.luc2 and Ad.luc2 into nude mice bearing bone metastases resulted in uptake of the viruses into skeletal tumors, and induced significant inhibition of established bone metastases. Thus, liver-detargeted oncolytic adenovirus can be developed for the treatment of breast cancer bone metastasis.

Introduction

In the United States, breast cancer is the second leading cause of malignancy-related deaths among women (American Cancer Society, 2010). In advanced stages of breast cancer, a majority of the patients develop bone metastases resulting in bone pain, bone destruction, and eventual death (Coleman, 2001). Development of novel therapies for the treatment of breast cancer bone metastases is a major unmet need in medicine. Oncolytic adenoviruses have shown some promise as antitumor agents (Bischoff *et al.*, 1996; McCormick, 2005; de Vrij *et al.*, 2010). Our laboratory is interested in developing recombinant adenoviruses for targeting breast cancer bone metastases (Seth, 1999; Seth *et al.*, 2006; Hu *et al.*, 2010b). A key limitation of systemic administration of adenovirus 5 (Ad5), however, is the liver sequestration of adenovirus, causing liver damage and necessitating the need to develop liver-detargeted oncolytic adenoviruses (Roberts *et al.*, 2006; Waddington *et al.*, 2008). Studies have shown that binding of blood coagulation factors, particularly factor X (FX), to the seven hypervariable regions (HVRs) of Ad5 hexon protein could result in the liver uptake of Ad5 (Parker *et al.*, 2006; Kalyuzhniy *et al.*, 2008; Waddington *et al.*, 2008; Alba *et al.*, 2009). Given that adenovirus serotype Ad48 has reduced hexon–FX binding capacity (Roberts *et al.*, 2006; Waddington *et al.*, 2008), we have generated a hexon-chimeric oncolytic adenovirus, mHAd.luc2, in which the HVRs of Ad5 were substituted with those of Ad48. We have examined whether mHAd.luc2 would have reduced liver uptake, and be safer than the parental Ad.luc2, while maintaining antitumor efficacy against breast cancer bone metastasis.

Gene Therapy Program, Department of Medicine, NorthShore Research Institute, an affiliate of the University of Chicago, Evanston, IL 60201.

Materials and Methods

Cell lines

MDA-MB-231-luc2 cells were generated by stably transfecting human breast cells MDA-MB-231 with pGL4.17cmv-luc2 (Promega, Madison, WI). Human breast cancer cells MDA-MB-231 and MCF-7, and HEK293 cells, were grown as described previously (Katayose *et al.*, 1995; Hu *et al.*, 2010b).

Adenoviral vectors

mHAd.luc2 containing chimeric hexon of Ad5 and Ad48 was created as described in Results and Discussion. Ad.luc2 and mHAd.luc2 are oncolytic adenoviral vectors derived from adenoviral mutant *dl*01/07 (Howe *et al.*, 2000) with two deletions in the E1A region; the *luc2* gene was cloned in the E3 region, but the adenoviral death protein sequence was left intact. Ad(E1–).luc2 is a replication-deficient vector with the *luc2* gene inserted in the E3 region. Adenoviruses were propagated and purified as described earlier (Katayose *et al.*, 1995).

Bioluminescence imaging of liver gene transduction

All animal experimental procedures were approved by the Institutional Animal Care and Use Committee of the NorthShore University HealthSystem (Evanston, IL). Six-week-old female athymic *nu/nu* mice (Charles River Laboratories, Wilmington, MA) were injected intravenously with Ad.luc2 or mHAd.luc2 (5.0×10^{10} viral particles [VP]/mouse). Whole body bioluminescence imaging (BLI) was performed, and images were processed with an IVIS-200 spectrum system (Caliper Life Sciences, Hopkinton, MA). The kinetics of liver gene transduction were monitored for 30 days.

Liver toxicity studies

Six-week-old female nude mice were injected with Ad.luc2 or mHAd.luc2 (low dose [LD], 5.0×10^{10} VP/mouse; high dose [HD], 1.0×10^{11} VP/mouse) via the tail vein. Three days after virus injection, liver genomic DNA was extracted, using a QIAamp kit (Qiagen, Valencia, CA). Viral genome copies were measured by quantitative PCR (qPCR) using forward primer cagcgtagccccgatgtaag and reverse primer tttttgagc agcaccttgca. Liver alanine transaminase (ALT) levels were measured with an ALT assay kit (Cayman Chemical, Ann Arbor, MI). Liver tissues were collected and processed for hematoxylin and eosin (H&E) staining.

Virus-binding and viral replication assays

For the virus-binding assay, MDA-MB-231 cells were plated in 24-well plates at 1×10^5 cells per well. The next day, cells were washed three times with ice-cold phosphate-buffered saline (PBS) and incubated at 4°C with adenovirus (2.5×10^4 VP/cell) with or without FX (10 μg/ml). After 1 hr, viral genomic DNA was quantified by qPCR. For the viral replication assay, MDA-MB-231 cells were infected with adenoviral vector (2.5×10^4 VP/cell). Viral titers of 3- and 48-hr samples were determined with an adenoviral kit (Clontech, Mountain View, CA). Viral burst size was calculated by dividing viral titers of 48-hr samples by that of 3-hr samples as described earlier (Hu *et al.*, 2010a).

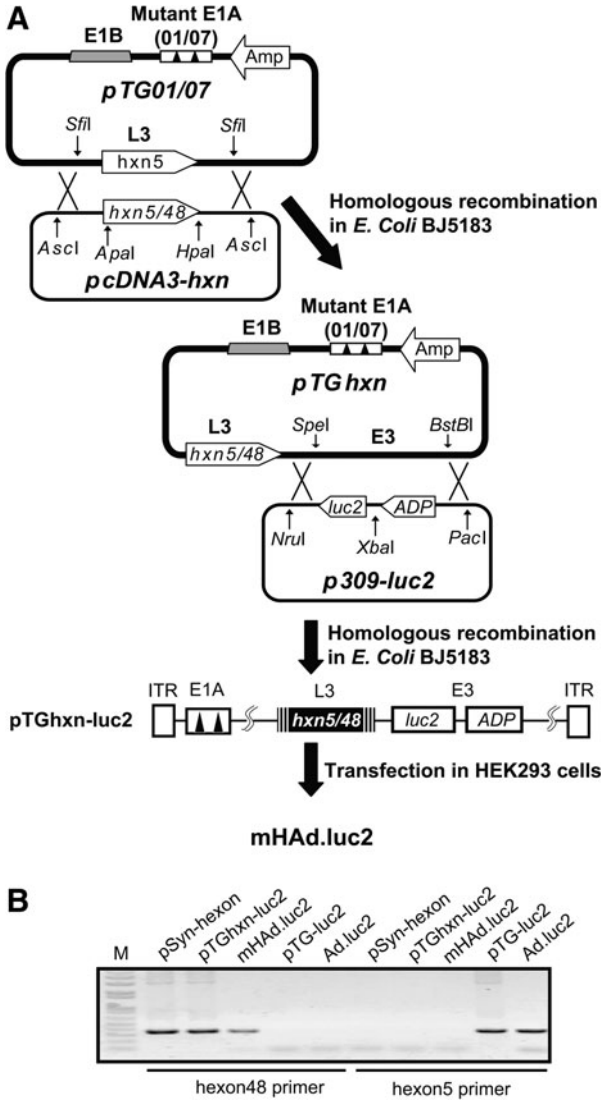

FIG. 1. Construction of hexon-chimeric adenovirus mHAd.luc2. **(A)** Construction of mHAd.luc2. A partial Ad5 hexon gene containing the hypervariable regions (HVRs) (0.7 kb) from Ad48 was chemically synthesized. The gene was cloned as *Apa*I–*Hpa*I fragments into the plasmid containing the complete Ad5 hexon gene to create the shuttle plasmid pcDNA3-hxn. An *Asc*I–*Asc*I fragment excised from pcDNA3-hxn was cotransformed with *Sfi*I-digested pTG01/07 in *Escherichia coli* BJ5183, to produce hexon-chimeric viral backbone DNA pTGhxn. Homologous recombination between a *Pac*I–*Nru*I fragment from p309-luc2 and a *Spe*I–*BstB*I fragment from pTGhxn produced viral genomic DNA pTGhxn-luc2. The *Pac*I-digested pTGhxn-luc2 was transfected into HEK293 cells to produced mHAd.luc2. **(B)** Replacement of the HVRs of Ad5 hexon with those of Ad48 was confirmed by PCR amplification using two pairs of primers targeting Ad5 or Ad48 hexon sequence. Primers were as follows: common forward primer, acaggggccctactttaag; reverse primer targeting Ad5 hexon, ttaggtgtttgaccttcg; reverse primer targeting Ad48 hexon, atcttcctctttggttgc. Synthesized Ad48 hexon sequence (pSyn-hxn), viral genomic DNA (pTGhxn-luc2), and purified mHAd.luc2 were detected with Ad48 hexon primers, but not those of Ad5 hexon. Parental viral DNA pTG-luc2 and Ad.luc2 were used as controls. M, DNA marker.

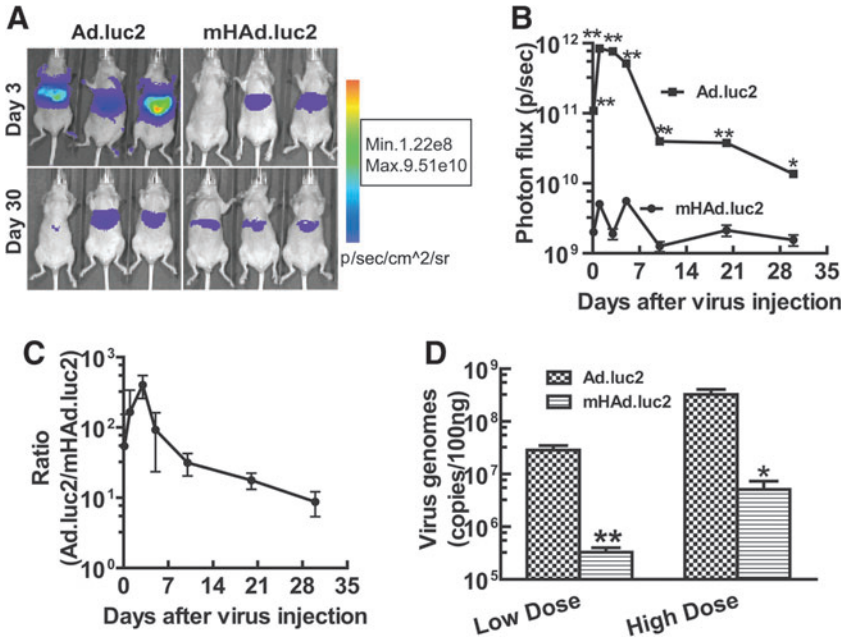

FIG. 2. mHAd.luc2 exhibits reduced liver uptake of virus compared with Ad.luc2. **(A)** Ad.luc2 or mHAd.luc2 (5.0×10^{10} VP/mouse) was injected into mice via the tail vein. Bioluminescence imaging was performed at various time points. Representative images on days 3 and 30 are shown. **(B)** The kinetics of liver gene transduction on various days. **(C)** The ratio of luciferase expression between Ad.luc2 and mHAd.luc2 treatment groups on various days. **(D)** Viral genomic copies in mouse liver 3 days after intravenous injection of virus (low dose [LD], 5.0×10^{10} VP/mouse; high dose [HD], 1.0×10^{11} VP/mouse). For (**A**–**D**), $n=6$ mice per group. $^{*}p<0.05$; $^{**}p<0.01$.

Examining viral uptake in skeletal tumors

MDA-MB-231 cells were inoculated into the left ventricle of nude mice (1.5×10^{5} per mouse, in 100 μl of PBS) as described earlier (Yin *et al.*, 1999; Hu *et al.*, 2010b). Mice with X-ray-positive skeletal lesions (15 days after tumor cell injection) were injected with Ad.luc2 or mHAd.luc2 (5.0×10^{10} VP in 0.1 ml of buffer) via the tail vein. Three days later, BLI of the hind limbs was performed to measure viral uptake in skeletal tumors.

Effect of adenoviral vectors on the progression of bone metastasis

MDA-MB-231-luc2 cells (1.5×10^{5} per mouse, in 100 μl of buffer) were inoculated into the left ventricle of nude mice (day 0). On day 8, mice were subjected to BLI imaging, and split into four groups (with no significant difference in luminescence intensity within each group). Mice were administered either buffer, Ad(E1–).luc2, Ad.luc2, or mHAd.luc2 via tail vein injection on days 9, 12, and 15 (2.5×10^{10} VP/dose per

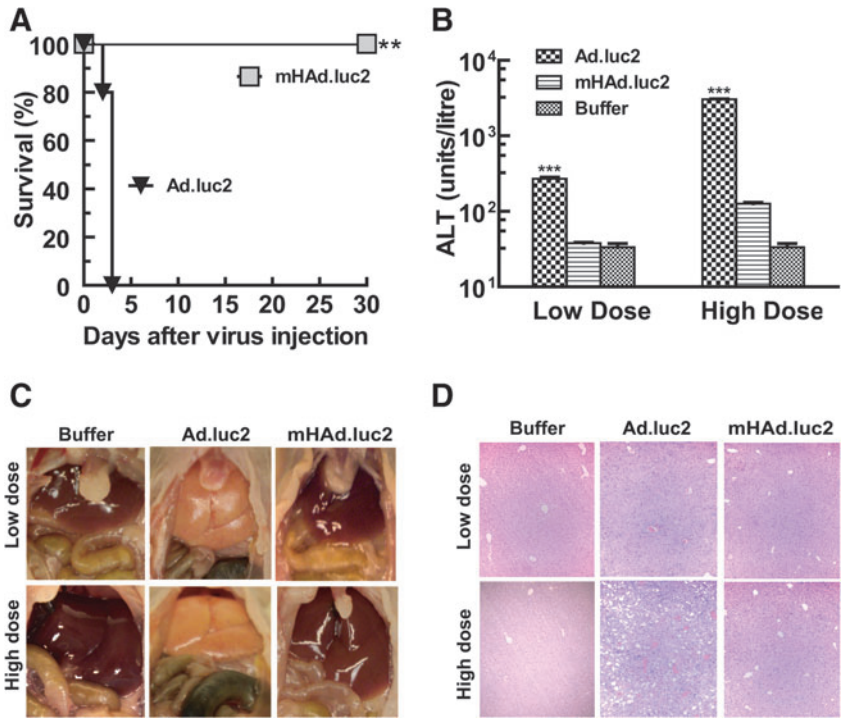

FIG. 3. mHAd.luc2 exhibits reduced liver toxicity compared with Ad.luc2. **(A)** Survival of mice after intravenous injection of a high viral dose (1×10^{11} VP/mouse). Mice were monitored for 30 days, and killed once significant signs of morbidity/mortality were observed $^{**}p<0.01$. **(B)** Liver serum ALT levels from the high-dose and low-dose groups. $^{***}p<0.001$. **(C)** Representative *in situ* photographs of liver after systemic delivery of viruses. (**A**–**C**, $n=6$ mice in each group.) **(D)** Livers were harvested and processed for hematoxylin and eosin (H&E) staining (day 3 samples). A representative example (×100) from each treatment group is shown.

mouse, in 100 μl of buffer). X-ray radiographs of mice in the prone position were obtained with an LX-60 system (Faxitron, Lincolnshire, IL). The osteolytic lesion areas in hind limbs were quantified on days 12, 16, and 22, using ImageJ software (National Institutes of Health). The experiment was terminated because of mouse death/sickness in control group.

Statistical analyses

Data are presented as means ± SEM. Statistical analyses were performed with GraphPad Prism software version 5 (GraphPad Software, San Diego, CA). Two-way repeated-measures analysis of variance (ANOVA) followed by Bonferroni post tests was used to analyze tumor progression. Survival data were analyzed by log-rank test. The Student *t* test was conducted to determine the significance of differences between two groups. $p < 0.05$ was considered significant.

Results and Discussion

mHAd.luc2 containing chimeric hexon of Ad5 and Ad48 was created by swapping the Ad48 hexon sequence, between *Apa*I and *Hpa*I restriction sites, for the corresponding hexon sequence in Ad5 (Fig. 1A). PCR amplification assay shows the presence of Ad48 HVRs in mHAd.luc2 (Fig. 1B).

To investigate the liver uptake of mHAd.luc2 and Ad.luc2, viral vectors were injected into nude mice via the tail vein (5.0×10^{10} VP/mouse). At various time points (up to 30 days), mice were subjected to BLI. Examples of BLI on days 3 and 30 of three mice in each group are shown (Fig. 2A). Total light emission in the liver was calculated and plotted as a function of time (Fig. 2B). Luciferase expression in the mHAd.luc2 group was significantly lower than in the Ad.luc2 group (at each time point, $p < 0.01$; except on day 30, $p < 0.05$). On day 3, an approximately 400-fold reduction in luciferase expression was observed (Fig. 2C). In a separate experiment, the presence of adenoviral vector in mouse liver was measured by qPCR, 3 days after intravenous injection of viral vectors. Viral DNA was significantly lower in the mHAd.luc2 group compared with the Ad.luc2 group (Fig. 2D, $p < 0.01$, LD group; $p < 0.05$, HD group), indicating that hexon modification resulted in the reduction of mHAd.luc2 liver uptake.

To further compare the safety and toxicity of Ad.luc2 and mHAd.luc2, viruses were systemically injected into mice. Mice were monitored for 30 days for signs of morbidity, and liver damage was evaluated. All mice in the Ad.luc2 HD group showed significant morbidity/mortality and were killed on day 3. In the mHAd.luc2 HD group, mice remained active during the course of the experiment (Fig. 3A; $p < 0.01$, log-rank test). Serum alanine transaminase (ALT) levels in the Ad.luc2 group were significantly higher than in the mHAd.luc2 group (Fig. 3B; LD, $p < 0.001$; HD, $p < 0.001$). Livers in the Ad.luc2 group were pale/yellow in appearance, whereas livers from the mHAd.luc2 or buffer group had a normal bright red appearance (Fig. 3C). Ad.luc2 (HD group) exhibited massive necrosis (Fig. 3D). No distinct morphological changes were observed in the mHAd.luc2 group compared with the buffer group (Fig. 3D). These results suggest that hexon replacement improved the *in vivo* safety profile of oncolytic adenovirus.

Considering our goal to create oncolytic adenoviruses for the treatment of breast cancer bone metastases, the effect of hexon modification on viral binding and replication in MDA-MB-231 cells *in vitro*, and viral uptake in skeletal tumors *in vivo*, were examined. In the absence of FX, similar binding of mHAd.luc2 and Ad.luc2 was observed (Fig. 4A, $p > 0.05$). However, in the presence of FX, as expected, mHAd.luc2 binding was lower than that of Ad.luc2 (Fig. 4A, $p < 0.05$). In the viral replication assay, there was no detectable viral replication of Ad(E1–).luc2, whereas both Ad.luc2 and mHAd.luc2 produced a burst size of about 400 (Fig. 4B, $p = 0.397$, Ad.luc2 vs. mHAd.luc2), indicating that hexon replacement did not affect the viral replication of oncolytic adenovirus. Next, we examined whether the systemic delivery of adenoviruses would result in the accumulation of viruses in skeletal tumors. Mice were injected with MDA-MB-231 cells via the intracardiac route. After 15 days, mice

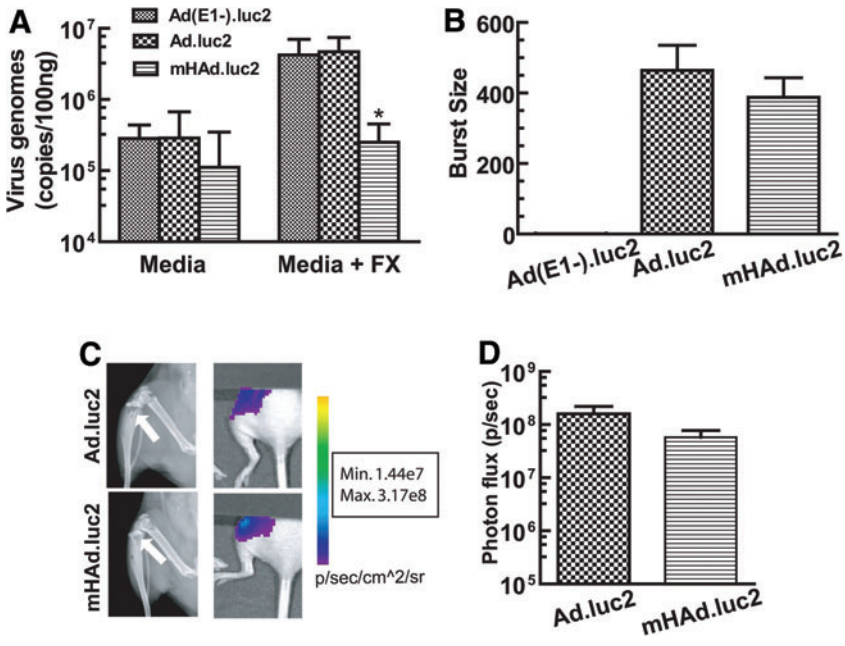

FIG. 4. Binding and replication of viral vectors *in vitro*, and uptake into skeletal tumors *in vivo*. **(A)** Viral binding with MDA-MB-231 cells *in vitro*. Cells were incubated with either serum-free medium or medium containing FX (10 μg/ml). Viral genomic copies were determined by qPCR. *$p < 0.05$ compared with Ad.luc2. **(B)** Viral replication assay showing the burst sizes of mHAd.luc2 and Ad.luc2 in MDA-MB-231 cells. Data are representative of three independent experiments. **(C)** Virus uptake in skeletal tumors *in vivo*. MDA-MB-231 cells were inoculated into the left heart ventricle to establish bone metastasis. Mice with X-ray-positive tumors (*left*, images on day 15) were administered virus (on day 15) via the tail vein. Three days later, bioluminescence imaging of the hind limbs was performed (*right*). **(D)** Quantification of the BLI signal in skeletal lesions (**C** and **D**, $n = 6$ mice per group). Color images available online at www.liebertonline.com/hum

bearing X-ray-positive bone lesions (Fig. 4C, left) were injected with mHAd.luc2 or Ad.luc2 via the tail vein. BLI examination of the hind limbs (BLI of the left limb, shown in Fig. 4C, right) was examined. The quantification of BLI signal indicated that both viruses produced nearly equal levels of vector-induced luciferase expression in skeletal tumors (Fig. 4D) ($p > 0.05$), indicating that hexon modification did not affect the uptake of virus into skeletal tumors.

To examine the therapeutic efficacy of mHAd.luc2, MDA-MB-231-luc2 cells were injected into the left heart ventricle of nude mice to establish bone metastases. On day 8, mice bearing BLI-positive bone metastasis (Fig. 5A, left, shows a representative mouse from each group) were divided randomly into four groups (there was no significant difference between the BLI intensity amongst the various groups). Mice were given three injections of either buffer, Ad(E1–).luc2, Ad.luc2, or mHAd.luc2. Tumor lesion areas were measured by X-ray radiography on days 12, 16, and 22. Mice that received mHAd.luc2 or Ad.luc2 had significantly smaller tumors compared with the buffer group or the replication-deficient Ad(E1–).luc2 virus group (Fig. 5A, right, and Fig. 5B; $p < 0.05$). Tumor lesion areas in the mHAd.luc2 and Ad.luc2 groups were similar (Fig. 5B, $p = 0.801$), indicating that hexon modification in mHAd.luc2 did not compromise the antitumor effect of the oncolytic virus.

In summary, the work presented here shows that hexon-chimeric mHAd.luc2 exhibits reduced liver uptake and reduced liver damage, and is safer than the unmodified Ad.luc2 virus. Systemic administration of mHAd.luc2 results in viral uptake in the tumors at the bone site, and the virus is quite effective in producing antitumor effects against established bone metastasis. It is interesting that *in vitro*, in the presence of factor X, compared with mHAd.luc2, unmodified Ad.luc2 can bind more to the tumor cells. However, the replication potential of mHAd.luc2 is not compromised. Moreover, both mHAd.luc2 and Ad.luc2 are equally effective in their uptake in tumors *in vivo*, and in producing antitumor responses against established bone metastases. Considering the superior safety profile of mHAd.luc2 compared with Ad.luc2, it would be interesting to examine in future whether increasing the viral dose to the maximal tolerated dose can improve the antitumor responses described here.

Oncolytic adenoviruses have emerged as an important class of antitumor agents (Crompton and Kirn, 2007; Yamamoto and Curiel, 2010). Systemic delivery of adenoviruses, however, faces a key *in vivo* barrier—the majority of the virus is taken up by the liver. It is known that intravenous delivery of Ad5 results in its uptake in the liver hepatocytes, a process that has been shown to be mediated via vitamin K-dependent FX binding with hexon (Parker *et al.*, 2006; Kalyuzhniy *et al.*, 2008; Waddington *et al.*, 2008; Alba *et al.*, 2009). Consistent with this is the observation that warfarin, a known inhibitor of FX biosynthesis, can inhibit Ad5 uptake in the liver, and enhance antitumor efficacy after systemic delivery (Shashkova *et al.*, 2008). Systemic delivery of Ad5 also results in sequestration by Kupffer cells through a nonspecific scavenger receptor pathway (Prill *et al.*, 2011). Several factors including immunoglobulin M, the complement system, and other blood components have also been shown to be involved in virus uptake in the liver (Xu *et al.*, 2008). It is, therefore, quite interesting that substituting the seven HVRs of Ad5 hexon with Ad5/48 chimeric hexon can have such a profound effect on

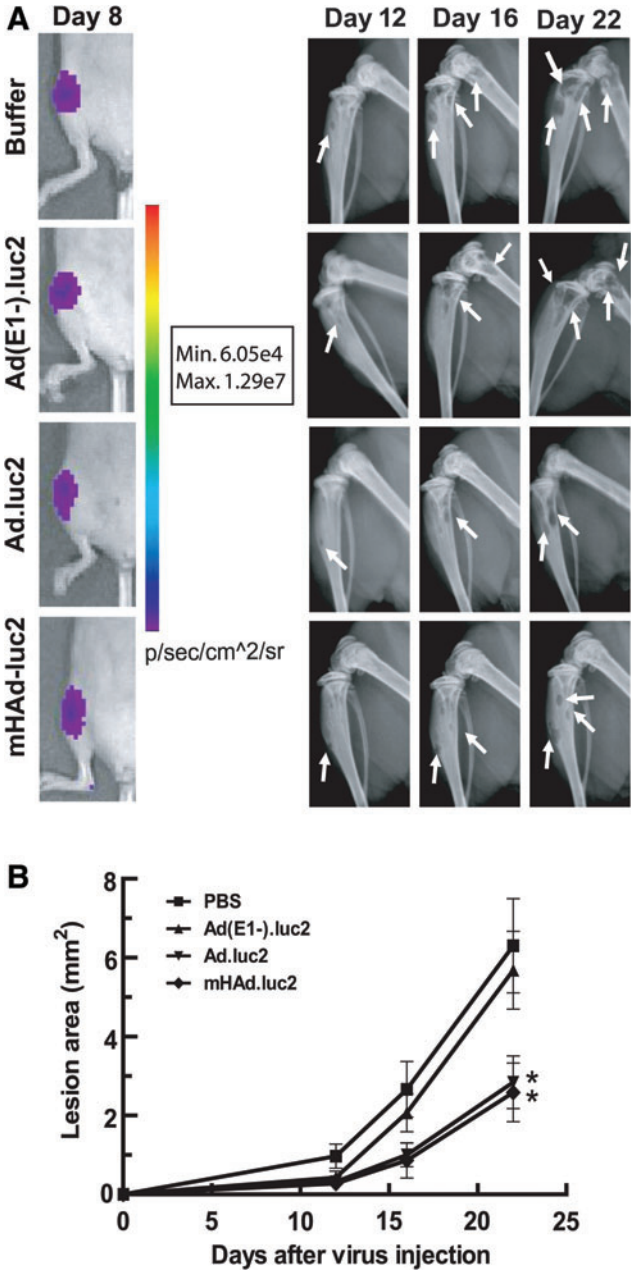

FIG. 5. Ad.luc2 and mHAd.luc2-mediated inhibition of established bone metastasis. (**A**) MDA-MB-231-luc2 cells were injected (day 0) into the left ventricle to establish bone metastasis in nude mice. On day 8, mice were subjected to bioluminescence imaging (*left*). Mice with detectable signals on hind limbs were randomized into four groups and injected with adenoviral vector on days 9, 12, and 16. X-ray radiographs of hind limbs on days 12, 16, and 22 are shown (*right*). (**B**) Osteolytic lesion areas in hind limbs on various days. *$p < 0.05$ compared with buffer group. (**A** and **B**, $n = 10$ mice per group). Color images available online at www.liebertonline.com/hum

the inhibition of viral uptake by the liver, without affecting viral uptake in the skeletal tumors. It is noteworthy that an oncolytic adenovirus in which Ad5 hexon was substituted with Ad3 hexon has been shown to be detargeted for liver, but is effective in inhibiting subcutaneous tumors in a mouse

model (Short *et al.*, 2010). It is possible that, on systemic delivery of mHAd.luc2 in mice bearing preestablished bone metastases as described here, relatively poor uptake of mHAd.luc2 (compared with Ad.luc2) in the liver, particularly during the initial 3 days, can result in higher mHAd.luc2 levels in the blood. This could result in higher blood levels of mHAd.luc2, thus favoring mHAd.luc2 accumulation in skeletal tumors *in vivo* in amounts that are similar to Ad.luc2. Once the hexon-modified virus reaches the target site, it elicits the expected oncolytic effects against the bone metastases. The evaluation of this hypothesis or other possible mechanisms to understand the *in vivo* antitumor responses of Ad5/48 chimeric hexon-based oncolytic adenovirus will be the focus of future investigation. It is quite significant, however, that Ad5/48 chimeric hexon-based liver-detargeted oncolytic adenoviruses could be potentially developed as a safe and effective approach for the systemic treatment of breast cancer bone metastasis.

Acknowledgments

This work was supported by National Institutes of Health grant R01CA127380 (P.S.). The authors thank Dr. Janardan Khandekar, Maxine and James Farrell, the Carol Gollob Foundation, and an anonymous source for their generous support. The authors thank Rebecca Orr for help in tissue processing, and Dr. Theresa Guise for providing the MDA-MB-231 cell line.

Author Disclosure Statement

No competing financial interests exist for any of the authors.

References

Alba, R., Bradshaw, A.C., Parker, A.L., *et al.* (2009). Identification of coagulation factor (F)X binding sites on the adenovirus serotype 5 hexon: Effect of mutagenesis on FX interactions and gene transfer. Blood 114, 965–971.

American Cancer Society. (2010). *Cancer Facts and Figures 2010* (American Cancer Society).

Bischoff, J.R., Kirn, D.H., Williams, A., *et al.* (1996). An adenovirus mutant that replicates selectively in p53-deficient human tumor cells. Science 274, 373–376.

Coleman, R.E. (2001). Metastatic bone disease: Clinical features, pathophysiology and treatment strategies. Cancer Treat. Rev. 27, 165–176.

Crompton, A.M., and Kirn, D.H. (2007). From ONYX-015 to armed vaccinia viruses: The education and evolution of oncolytic virus development. Curr. Cancer Drug Targets 7, 133–139.

de Vrij, J., Willemsen, R.A., Lindholm, L., *et al.* (2010). Adenovirus-derived vectors for prostate cancer gene therapy. Hum. Gene Ther. 21, 795–805.

Howe, J.A., Demers, G.W., Johnson, D.E., *et al.* (2000). Evaluation of E1-mutant adenoviruses as conditionally replicating agents for cancer therapy. Mol. Ther. 2, 485–495.

Hu, Z., Robbins, J.S., Pister, A., *et al.* (2010a). A modified hTERT promoter-directed oncolytic adenovirus replication with concurrent inhibition of TGFβ signaling for breast cancer therapy. Cancer Gene Ther. 17, 235–243.

Hu, Z., Zhang, Z., Guise, T., and Seth, P. (2010b). Systemic delivery of an oncolytic adenovirus expressing soluble transforming growth factor-β receptor II–Fc fusion protein can inhibit breast cancer bone metastasis in a mouse model. Hum. Gene Ther. 21, 1623–1629.

Kalyuzhniy, O., Di Paolo, N.C., Silvestry, M., *et al.* (2008). Adenovirus serotype 5 hexon is critical for virus infection of hepatocytes *in vivo*. Proc. Natl. Acad. Sci. U.S.A. 105, 5483–5488.

Katayose, D., Gudas, J., Nguyen, H., *et al.* (1995). Cytotoxic effects of adenovirus-mediated wild-type p53 protein expression in normal and tumor mammary epithelial cells. Clin. Cancer Res. 1, 889–897.

McCormick, F. (2005). Future prospects for oncolytic therapy. Oncogene 24, 7817–7819.

National Institutes of Health. *ImageJ*. (U.S. National Institutes of Health, Bethesda, MD). Available at http://rsb.info.nih.gov/ij/

Parker, A.L., Waddington, S.N., Nicol, C.G., *et al.* (2006). Multiple vitamin K-dependent coagulation zymogens promote adenovirus-mediated gene delivery to hepatocytes. Blood 108, 2554–2561.

Prill, J.M., Espenlaub, S., Samen, U., *et al.* (2011). Modifications of adenovirus hexon allow for either hepatocyte detargeting or targeting with potential evasion from Kupffer cells. Mol. Ther. 19, 83–92.

Roberts, D.M., Nanda, A., Havenga, M.J., *et al.* (2006). Hexon-chimaeric adenovirus serotype 5 vectors circumvent pre-existing anti-vector immunity. Nature 441, 239–243.

Seth, P., ed. (1999). *Adenoviruses: Basic Biology to Gene Therapy* (R.G. Landes, Austin, TX).

Seth, P., Wang, Z.G., Pister, A., *et al.* (2006). Development of oncolytic adenovirus armed with a fusion of soluble transforming growth factor-β receptor II and human immunoglobulin Fc for breast cancer therapy. Hum. Gene Ther. 17, 1152–1160.

Shashkova, E.V., Doronin, K., Senac, J.S., and Barry, M.A. (2008). Macrophage depletion combined with anticoagulant therapy increases therapeutic window of systemic treatment with oncolytic adenovirus. Cancer Res. 68, 5896–5904.

Short, J.J., Rivera, A.A., Wu, H., *et al.* (2010). Substitution of adenovirus serotype 3 hexon onto a serotype 5 oncolytic adenovirus reduces factor X binding, decreases liver tropism, and improves antitumor efficacy. Mol. Cancer Ther. 9, 2536–2544.

Waddington, S.N., McVey, J.H., Bhella, D., *et al.* (2008). Adenovirus serotype 5 hexon mediates liver gene transfer. Cell 132, 397–409.

Xu, Z., Tian, J., Smith, J.S., and Byrnes, A.P. (2008). Clearance of adenovirus by Kupffer cells is mediated by scavenger receptors, natural antibodies, and complement. J. Virol. 82, 11705–11713.

Yamamoto, M., and Curiel, D.T. (2010). Current issues and future directions of oncolytic adenoviruses. Mol. Ther. 18, 243–250.

Yin, J.J., Selander, K., Chirgwin, J.M., *et al.* (1999). TGF-β signaling blockade inhibits PTHrP secretion by breast cancer cells and bone metastases development. J. Clin. Invest. 103, 197–206.

Address correspondence to:
Dr. Prem Seth
Gene Therapy Program
NorthShore Research Institute
2650 Ridge Avenue, Room B 652
Evanston, IL 60201

E-mail: pseth@northshore.org *or* pseth@uchicago.edu

Received for publication April 11, 2011;
accepted April 12, 2011.

Published online: April 12, 2011.